BMB
reports

Detection for folding of the thrombin binding aptamer using label-free electrochemical methods

Minseon Cho[1], Yeonwha Kim[1], Se-Young Han[1], Kyungin Min[1], Md. Aminur Rahman[2], Yoon-Bo Shim[2] & Changill Ban[1,]*

[1]Department of Chemistry, Pohang University of Science and Technology, Pohang, [2]Department of Chemistry, Pusan National University, Busan, Korea

The folding of aptamer immobilized on an Au electrode was successfully detected using label-free electrochemical methods. A thrombin binding DNA aptamer was used as a model system in the presence of various monovalent cations. Impedance spectra showed that the extent to which monovalent cations assist in folding of aptamer is ordered as $K^+ > NH_4^+ > Na^+ > Cs^+$. Our XPS analysis also showed that K^+ and NH_4^+ caused a conformational change of the aptamer in which it forms a stable complex with these monovalent ions. Impedance results for the interaction between aptamer and thrombin indicated that thrombin interacts more with folded aptamer than with unfolded aptamer. The EQCM technique provided a quantitative analysis of these results. In particular, the present impedance results showed that thrombin participates a folding of aptamer to some extent, and XPS analysis confirmed that thrombin stabilizes and induces the folding of aptamer. [BMB reports 2008; 41(2): 126-131]

INTRODUCTION

Nucleic acids play a central role in cellular processes, including recombination, transcription, translation, and ligand binding. These functions are largely determined by the particular three-dimensional structures of functional nucleotide molecules, as in the folding and unfolding of DNAs or RNAs. Details of the folding of DNAs or RNAs improve our understanding of their biological nature. In addition, this folding process is important in that misfolding of biomolecules causes conformational diseases (1). The discovery of chromosomal ended sequences, telomeres, has led to investigations of the formation of particular DNA structures (2). These sequences form a G-quadruplex stabilized by cyclic hydrogen bonding of four guanines. These are highly stable structures with metal ions coordinating between adjacent stacks of G-tetrads (3). G-quadruplexes are also commonly found in DNA aptamers (4). Quadruplexes depend for their formation and stability on tight binding of specific metal ions (5). In general, the presence of potassium ions gives more stable quadruplexes than other univalent cations (6, 7). According to CD spectra and UV melting techniques, cations with an ionic radius in the range 1.3-1.5 Å fit well within the two G-quartets of the complex, whereas other cations cannot (4). It has been also known that the thrombin aptamer folds into stable intramolecular G-quadruplex in the presence of Rb^+, NH_4^+, Sr^{2+} or Ba^{2+} as with K^+. However, the cations Li^+, Na^+, Cs^+, Mg^{2+} and Ca^{2+} form weaker complex (4).

In addition to the high affinity of aptamers to their target originated by their ability of folding, aptamers have a number of advantages surpassing antibodies. Unlike antibodies, aptamers are chemically synthesized, easily modified and relatively free from pH, temperature or buffer conditions. Moreover, aptamers have small size and are stable to long-term storage (6, 8, 9). Due to all these characteristics, recent years have seen various detection methods for aptamer sensors, such are optical (10-12) fluorescence (9, 13-15), quartz crystal microbalance (QCM) (16, 17) and electrochemical (6, 18-24) methods. In particular, impedance spectroscopy is a powerful technique for detecting the interaction between various biomolecules appearing at the surface of an electrode (25-27) This measurement has yielded sensitive and selective results for sensing aptamer and monitoring protein-aptamer interaction. X-ray photoemission spectroscopy (XPS) is also an immense influential label-free technique used to determine atomic compositions and learn information about the types of bonding that occurs within various compounds. One of the most valuable features of XPS is its ability to distinguish different chemical bonding configurations as well as different elements. The bonding energies of electrons in an atom are affected by the atom's chemical environments. These capabilities of XPS offer chemical information that favors the identification of biomolecules at a surface and the changing of their conformations (28).

Here, we have detected with impedance that the folding and unfolding state of G-quadruplex forming DNA aptamer which is changed according to surrounding environments. EQCM analysis was also conducted to support the folding effect of thrombin aptamer. In addition, XPS was used to analy-

*Corresponding author. Tel: 82-54-279-2127; Fax: 82-54-279-3399; E-mail: ciban@postech.ac.kr

Received 3 August 2007, Accepted 5 October 2007

Keywords: Aptamer folding, Impedance, Thrombin, Thrombin aptamer, XPS

sis the changes of aptamer conformation. The high affinity of aptamers for their targets is determined by their folding capability after binding their target molecules (29, 30). Therefore, detection for folding and unfolding conformation of aptamers is extremely important in that this makes it possible the development of affinity-based detection systems or even their use as chemotherapeutic agents, therapeutic tools and in clinical diagnostics.

RESULTS AND DISCUSSION

Folding effect of thrombin aptamer according to monovalent cations

5'-end thiol modified DNA aptamer (0.5 μM) was initially immobilized on an Au electrode at room temperature. Next, β-mercaptoethanol (β-ME) was used to eliminate non-bounded aptamer on Au surface so that a good monolayer could self-assemble, and thrombin was formed as a complex with the aptamer. Each immobilized state was detected by observing the change of charge transfer resistance (R_{ct}) in a Nyquist plot (Fig. 1A) (20).

To detect the folding effect of thrombin aptamer in the presence of monovalent cation, the impedance was measured with various monovalent cations: K^+, NH_4^+, Na^+ and Cs^+. These monovalent cations were chosen to have similar ionic strength, so we could confirm that the conductivity of the buffer does not influence the R_{ct} value. In fact, no change of R_{ct} values was observed using a bare Au electrode with buffers including different cations (data not shown). According to previous report, the folding effect of thrombin aptamer was dependent on increasing concentration of K^+ ions, and folding of aptamer was even detected in 0.1 mM K^+ (20). Our results show that the folding and unfolding behavior according to various monovalent cations can be detected through the R_{ct} values (Fig. 1B). In the presence of 100 mM K^+, the electron transfer resistance (R_{ct}) is higher (1783.8 Ω) than with other cations. In the other hands, it takes its lowest value in the presence of Cs^+ (499.78 Ω). Table 1 shows that R_{ct} values were influenced by aptamer folding after β-ME treatment as well, indicating non-specifically adsorbed aptamer is removed from the surface and that completely folded aptamer has high R_{ct} and weakly folded aptamer has low R_{ct}. This implies that the formation of G-quadruplex enhances resistance electron transfer and causes a further increase in R_{ct} values (20). According

Table 1. Values of R_{ct}, R_{ct} change values and change ratio of R_{ct} values according to concentration of thrombin

	KCl	NH_4Cl	NaCl	CsCl
R_{ct} (Ω)				
β-ME	361.5 ± 23.1	188.1 ± 16.4	166.9 ± 10.2	109.4 ± 7.8
%(ΔR_{ct})				
0.1 nM	286	196	167	165.7
0.5 nM	497	296	286	318.7
1 nM	602.6	500	470.5	401.8
10 nM	753	764	652	496.4
50 nM	994.9	972	798	630.8

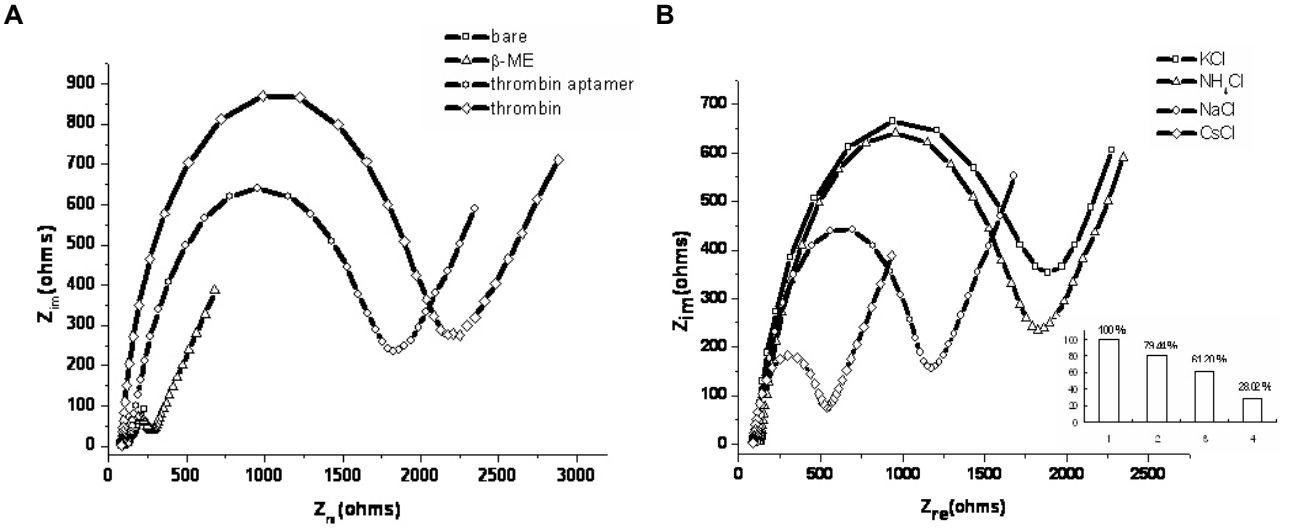

Fig. 1. (A) Nyquist plots for each step in the presence of 5 mM $Fe(CN)_6^{3-/4-}$. After immobilization of thrombin aptamer, R_{ct} was increase, and then, treatment of β-ME caused a decrease of R_{ct}. After interaction with thrombin, R_{ct} is re-increased due to interference of electron transfer. (B) Nyquist plots for detection of aptamer folding with different monovalent cations. Impedance spectra were recorded after immobilization of 0.5 μM aptamer in a 10 mM Cs-HEPES buffer (pH 7.4) including 5 mM $[Fe(CN)_6]^{3-/4-}$ and 100 mM monovalent cations. Bar plots for the relative aptamer folding in different buffers (inset).

to the impedance results, the extent to which monovalent cations assist in folding of aptamer is ordered as $K^+ > NH_4^+ > Na^+ > Cs^+$. One of the factors for determining this order is the ionic radius. The actual ionic radii in the range 1.3-1.5 Å are proper sizes for stabilizing a quadruplex (*e.g.*, K^+ (1.33 Å), NH_4^+ (1.43 Å), Na^+ (0.95 Å), Cs^+ (1.69 Å)) (4). Further, the hydration effects of cations could contribute the folding of a G quadruplex structure. The impedance spectra also contrast that high R_{ct} value of folded aptamer in KCl buffer with a much lower value upon changing to CsCl buffer. The opposite result is found for unfolded aptamer (data not shown). This observation implies that aptamer shielding cations were exchanged by cations in the buffer and that aptamers were influenced by surrounding cations in the buffer. It also follows that impedance measurement can reveal the folding of aptamer with different cations. Electrochemical reactions are inhibited at the electrode covered by aptamer (21). However, the present results suggest that electron transfer resistance on the electrode interface is also influenced by aptamer folding. The degree of aptamer folding was also related to the differing cations in NH_4Cl, NaCl and CsCl buffer, taking the R_{ct} value of thrombin aptamer in KCl buffer as corresponding to 100% folding (Fig. 1B inset). This plot shows that thrombin aptamer folds well in presence of NH_4^+ ion (79.44%), though folding effect was somewhat weak in comparison of K^+ ion, and Na^+ ion also affects the folding of aptamer (61.20%). However, thrombin aptamer scarcely folded in the presence of Cs^+ ion (28.02%).

CD spectroscopy confirmed the conformation of various aptamer-cation complexes (data not shown). All spectrums showed the similar shape, but the magnitude of maximum peaks was changed gradually at wavelength ~290-300 nm (4). The order of decrease was the same as the impedance results, $K^+ > NH_4^+ > Na^+ > Cs^+$, indicating that the K^+-aptamer complex folded well, but the Cs^+-aptamer complex scarcely folded.

XPS analysis was also carried out to confirm the effect of the various metal ions on the conformational change of the immobilized aptamer. XPS is a powerful tool to investigate the folding of aptamer, since chemical shifts of the XPS peak give much information about the chemical state of the molecule and changes in the molecular orientation. The survey spectra obtained for (a) a bare Au surface, (b) immobilization of a thiolated aptamer on an Au surface and the immobilized aptamer modified electrode after dipping into the solution containing Cs^+ (c), Na^+ (d), NH_4^+ (e), and K^+ (f) are also shown in Fig. S1A. The C1s peaks (Fig. 2Ac) at 284.6 eV, 286.5 eV, and 289.0 eV, which respectively corresponded to C-C, C-N, and C = O bonds, were not shifted to higher energies. Moreover, the N1s (Fig. S1Bc) and O1s peaks (Fig. 2Bc) appeared at similar energies those observed for an aptamer immobilized Au electrode. These results indicated that the Cs^+ ion could not affect a conformational change of the immobilized aptamer. For the Na^+ ion, chemical shifts were scarcely observed for the C1s, O1s, and N1s peaks. This implies that the Na^+ ion is able to cause weak folding of aptamer (Fig. 2Ad, 2Bd, and S1Bd). For NH_4^+ and K^+ ions, however, a slight shift of Au4f and S2p peaks was observed, but the C1s, N1s, and O1s peaks were significantly shifted to higher energies. The C1s peaks (Fig. 2Ae) at 284.6 eV, 286.5 eV, and 289.0 eV shifted to 285.5 eV, 287.0 eV, and 289.3 eV. The N1s (Fig. S1Be) and O1s peaks (Fig. 2Be) shifted to 400.3 eV and 401.2 eV, and 533.1 eV and 534.2 eV, respectively. These results indicate that NH_4^+ ion causes a conformational change of the immobilized aptamer by forming a stable complex between NH_4^+ and

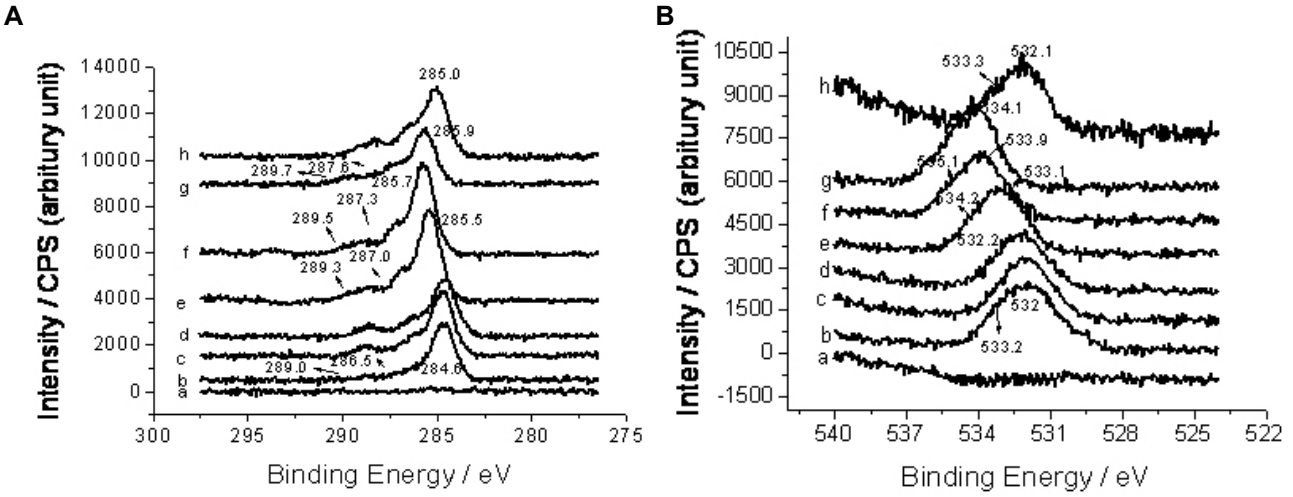

Fig. 2. XPS survey spectra (A) C1s peaks, and (B) O1s peaks obtained for (a) a bare Au surface, (b) after immobilization of a thiolated aptamer on an Au surface, (c-f) after dipping the aptamer immobilized Au surface into a solution containing Cs^+ (c), Na^+ (d), NH_4^+ (e), and K^+ (f), and after the interaction of thrombin with the immobilized aptamer that dipped in K^+ (g) and Cs^+ (h) solutions.

the aptamer. For the K^+ ion, the C1s peaks (Fig. 2Af) shifted to slightly higher energy, of 285.7 eV, 287.3 eV, and 289.5 eV, than those observed for the NH_4^+ ion. The N1s peaks (Fig. S1Bf) at 399.5 eV and 400.4 eV for $-NH_2$ and = NH bonds shifted to 400.7 eV and 401.5 eV, respectively. The O1s peaks (Fig. 2Bf) shifted to much higher energies to 533.9 eV and 535.1 eV, indicating that K^+ ion also caused a conformational change of the immobilized aptamer by forming a stable complex through coordination between K^+ and guanine carbonyl groups of the aptamer. The intensities of Cs3d and Na1s peaks were smaller than those of N1s and K2p peaks indicating that NH_4^+ and K^+ form a more stable complex than Cs^+ and Na^+. The greater energy shifts of C1s, N1s, and O1s peak in the case of K^+ ion, further indicated that K^+ ion forms a more stable complex than NH_4^+ ion. In summary, XPS analysis clearly supports the folding of thrombin aptamer according to monovalent cations, with the same results as impedance measurements.

Interaction between thrombin aptamer and thrombin

To measure the interaction between the folded aptamer and thrombin, thrombin (0.1, 0.5, 1, 10 and 50 nM) was incubated on aptamer modified electrode. With the buffer including KCl, a significant increase was observed in the R_{ct} value according to the increasing concentration of thrombin (Fig. S2A). The next highest R_{ct} values were observed for buffer including NH_4Cl and NaCl, respectively (data not shown). The lowest R_{ct} value was observed for buffer including CsCl (Fig. S2B). Thrombin could be detected down to a concentration of 0.1 nM. The change ratio of R_{ct} values (increased charge transfer resistance after interaction with thrombin/charge transfer resistance of thrombin aptamer × 100) was calculated, based on the detected R_{ct} (Table 1). The change ratio is very useful, because R_{ct} values are sensitive to the condition of the electrode surface; use of the ratio compensates for this factor. These results indicate that thrombin has more interactions with complete folded aptamers than with unfolded aptamers. To confirm this impedance results quantitatively, EQCM analysis was also carried out. In the presence of KCl or CsCl buffer, the amount of immobilized aptamer on the Au electrode was almost same (Table S1). This result shows that the amount of immobilized aptamer on the Au electrode is identical, regardless of the cation species. It constitutes direct verification that the different R_{ct} values are not due to the amount of immobilized aptamer, but are due to differences of aptamer folding. Table 1 also shows the amount of thrombin obtained after interaction with the aptamer. In the case of KCl buffer, the numbers of moles per unit electrode surface area were calculated to be 4.0×10^{-11} moles. This calculation means that the ratio of moles between aptamer and thrombin is almost 1 : 1 in aptamer-thrombin complex. In the case of CsCl buffer, the numbers of moles per unit electrode surface area were calculated to be almost half (2.26×10^{-11} mol) in comparison with KCl buffer. These results clearly showed that the amount of interacted thrombin depended on the aptamer folding influenced by the species of monovalent cation.

The effect of thrombin on folding of thrombin aptamer

It was found that thrombin has more interactions with complete folded aptamers than unfolded aptamers in Table 1 and Fig. S2. In addition, the $\%\Delta R_{ct}$ values in Table 1 suggest that interaction between thrombin and aptamer is influenced by the DNA folding. Fig. 3 shows the relative $\%\Delta R_{ct}$ values in presence of NH_4^+, Na^+, and Cs^+ ions, based on the $\%\Delta R_{ct}$ value in KCl buffer. In the case of NH_4Cl buffer, the relative $\%\Delta R_{ct}$ value was drastically increased in the presence of more than 1 nM thrombin. The aptamer has a folding ability by itself in presence of NH_4^+, with the relative folding value of 79.44% (Fig. 1B inset). Consequently, thrombin itself scarcely influences aptamer folding at low concentration (0.1 and 0.5 nM), but high concentrated thrombin (1, 10, 50 nM) does induce aptamer folding. A similar result was shown in NaCl buffer, because the Na^+-aptamer complex also has some folding ability (61.20%). On the other hand, the folding ability of aptamer was relatively weak in presence of Cs^+ ion (30.19%). So, the relative $\%\Delta R_{ct}$ value increased sharply at the lower concentration of thrombin (0.1 nM) in CsCl buffer. It therefore appears that thrombin assists folding of aptamer, a process which is also promoted by metal ions.

To confirm the effect of thrombin on folding of thrombin aptamer more clearly, XPS analysis was carried out with solutions containing K^+ and Cs^+ ion. Fig. 2 show the survey spectra by XPS. The C1s peaks obtained for the aptamer immobilized electrode dipping in a K^+ solution further shifted to higher energies to 285.9 eV, 287.6 eV, and 289.7 eV after throm-

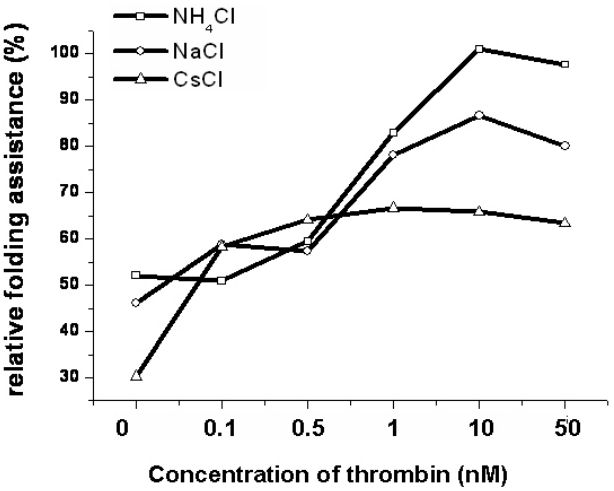

Fig. 3. Plots for relative folding (%) of aptamer with increasing concentration of thrombin (0.1, 0.5, 1, 10 and 50 nM) with buffers including different monovalent cations. Relative $\%\Delta R_{ct}$ values in presence of NH_4^+, Na^+, and Cs^+ ions were calculated, considering the R_{ct} value of thrombin aptamer in KCl buffer as 100% folding.

bin interaction (Fig. 2Ag). The N1s (Fig. S1Bg) peaks also shifted slightly to higher energies at 400.9 eV and 401.7 eV, respectively. However, the intensities of the N1s peaks increased significantly as a result of sufficient amino acid residues in thrombin. The O1s peaks (Fig. 2Bg) at 533.9 eV and 535.1 eV were found to be further shifted slightly to higher energies (534.1 eV and 535.3 eV) after thrombin interaction. These shifts of the C1s, N1s, and O1s peaks to higher energies show that thrombin interacts strongly with aptamer in a K^+ solution, and thrombin stabilizes the folded conformation of the aptamer. When the aptamer immobilized electrode dipped in a Cs^+ solution was interacted with thrombin, the C1s (Fig. 2Ah), N1s (Fig. S1Bh), and O1s (Fig. 2Bh) peaks did not shift to higher energies. Moreover, the intensities of the N1s peaks decreased. These results indicate that thrombin interacts weakly with the immobilized aptamer when the aptamer interacted Cs^+ ions, and high concentrated thrombin (10 nM) has a little effect on the conformational change of aptamer structure. Since high concentrated thrombin scarcely induced the folding of aptamer in CsCl buffer (Fig. 3), this finding is consistent with impedance data. When low concentration of thrombin (0.1 nM) was used, the chemical shift could not be detected in XPS analysis, due to the low signal-to-noise ratio (data not shown).

CONCLUSION

The folding of aptamer based on various monovalent cations was successfully detected using impedance spectroscopy and XPS. These results show that aptamer has different folding extent with different cations ($K^+ > NH_4^+ > Na^+ > Cs^+$). The folding effect of aptamer influences the interaction between thrombin and thrombin aptamer; this was confirmed by EQCM, quantitatively. In particular, all experiments in this study have meanings in that the folding and unfolding state of aptamer can be directly detected with a simple and label-free method. In addition, impedance data showed that thrombin assists folding of aptamer to some extent, and XPS analysis confirmed that interaction between thrombin and aptamer stabilizes the cation-aptamer complex and induces the folding of aptamer. This simple and label-free method for detecting the folding and unfolding conformation of aptamer can be a promising application for detecting the folding of biomolecules such as nucleotides or protein, and the interaction between various aptamer and their target proteins.

MATERIALS AND METHODS

Materials

The 5'-thiol modified thrombin binding aptamer (5'-HS-$(CH_2)_6$-GGTTGGTGTGGTTGG-3'), HPLC-purified, was purchased from Bioneer Inc (Korea). The modified aptamer was purified again using a reverse-phase chromatography column. Pure human thrombin was purchased from Haematologic Technologies Inc (USA).

Electrochemical measurements and X-ray photoemission spectroscopic analysis

Impedance was measured using a PARSTAT 2263 (USA) and spectra were collected at an open circuit voltage of 100 KHz down to 100 mHz (AC amplitude, 10 mV; sampling rate, 10 points per decade).

EQCM analysis was conducted with QCM 100 from Stanford Research System, USA. The working electrode for the EQCM experiments was a 5 MHz AT-cut quartz crystal with a gold electrode.

XPS experiments were performed using a VG scientific ESCA lab 250 XPS spectrometer with a monochromated AlK_α source with charge compensation in the Korea Basic Science Institute (Busan). Gold disks electrode (ca. 0.02 cm^2 geometrical area) were used for the XPS measurements.

Analytical procedures

The freshly cleaned gold electrode was incubated in 0.5 μM thiol-modified thrombin aptamer for 12 h at room temperature and 120 r.p.m. on a shaker. The β-mercaptoethanol (β-ME) treatment using 0.1 M solution in HEPES buffer was maintained for 1 min. This electrode was rinsed with HEPES buffer and subsequently incubated in different concentrations of thrombin for 30 min. This electrode was also rinsed with HEPES buffer for eliminating the unbound thrombin. Each step was confirmed by EQCM and impedance techniques.

Acknowledgements

The authors gratefully thank Professor Su-Moon Park for his constant support. This work was supported financially from Korea Health Industry Development Institute through Healthcare and Biotechnology Development Program (A050426) and KOSEF through the Center for Integrated Molecular System at POSTECH (R11-2000-070-070010).

Supplementary data

Supplementary data associated with this article can be found in the online version.

REFERENCES

1. Lee, C. and Yu, M.-H. (2005) Protein folding and diseases. *J. Biochem. Mol. Biol.* **38,** 275-280.
2. Greider, C. W. (1991) Telomeres. *Curr. Opin. Cell Biol.* **3,** 444-451.
3. Williamson, J. R., Rahguraman, M. K. and Cech, T. R. (1989) Monovalent cation-induced structure of telomeric DNA: The G-quartet model. *Cell* **59,** 871-880.
4. Kankia, B. I. and Marky, L. A. (2001) Folding of thrombin aptamer into a G-quadruplex with Sr^{2+}: stability, heat, and hydration. *J. Am. Chem. Soc.* **123,** 10799-10804.
5. Sharfer, R. H. and Smirnov, I. (2001) Biological aspects of DNA/RNA quadruplexes. *Biopolymers* **56,** 209-227.
6. Radi, A.-E., Sanchez, J. L. A., Baldrich, E. and O'Sullivan,

C. K. (2005a) Reagentless, reusable, ultrasensitive electrochemical molecular beacon aptasensor. *J. Am. Chem. Soc.* **128,** 117-124.
7. Ueyama, H., Takagi, M. and Takenaka, S. (2002) A novel potassium sensing in aqueous media with a synthetic oligonucleotide derivative. Fluorescence resonance energy transfer associated with guanine quartet-potassium ion complex formation. *J. Am. Chem. Soc.* **124,** 14286-14287.
8. Murphy, M. B., Fuller, S. T., Richardson, P. M. and Doyle, S. A. (2003) An improved method for the in vitro evolution of aptamers and applications in protein detection and purification. *Nucleic Acids Res.* **31,** e110.
9. Stadtherr, K., Wolf, H. and Lindner, P. (2005) A aptamer-based protein biochip. *Anal. Chem.* **77,** 3437-3443.
10. Jiang, Y., Fang, X. and Bai, C. (2004) Signaling aptamer/protein binding by a molecular light switch complex. *Anal. Chem.* **76,** 5230-5235.
11. Pavlov, V., Xiao, Y., Shlyabovsky, B. and Willner, I. (2004) Aptamer-functionalized Au nanoparticles for the amplified optical detection of thrombin. *J. Am. Chem. Soc.* **126,** 11768-11769.
12. Tombelli, S., Minunni, M. and Mascini, M. (2002) A surface plasmon resonance biosensor for the determination of the affinity of drugs for nucleic acids. *Anal. Lett.* **35,** 599-613.
13. Fang, X., Cao, Z., Beck, T. and Tan, W. (2001) Molecular aptamer for real-time oncoprotein platelet-derived growth factor monitoring by fluorescence anisotropy. *Anal. Chem.* **73,** 5752-5757.
14. Hamaguchi, N., Ellignton, A. and Stanton, M. (2001) Aptamer beacons for the direct detection of proteins. *Anal. Biochem.* **294,** 126-131.
15. Li, W., Wang, K., Tan, W., Ma, C. and Yang, X. (2007) Aptamer-based analysis of angiogenin by fluorescence anisotropy. *Analyst* **132,** 107-113.
16. Hianik, T., Ostatna, V., Zajacova, Z., Stoikova, E. and Evtugyn, G. (2005) Detection of aptamer-protein interactions using QCM and electrochemical indicator methods. *Bioorg. Med. Chem. Lett.* **15,** 291-295.
17. Liss, M., Petersen, B., Wolf, H. and Lindner, P. (2005) An aptamer-based quartz crystal protein biosensor. *Anal. Chem.* **74,** 4488-4495.
18. Hansen, J. A., Wang, J., Kawde, A.-N., Xiang, Y., Gothelf, K. V. and Collins, G. (2006) Quantum-dot/aptamer-based ultrasensitive multi-analyte electrochemical biosensor. *J. Am. Chem. Soc.* **128,** 2228-2229.
19. Ikebukuro, K., Kiyohara, C. and Sode, K. (2005) Novel electrochemical sensor system for protein using the aptamers in sandwich manner. *Biosens. Bioelectron.* **20,** 2168-2172.
20. Radi, A.-E. and O'Sullivan, C. K. (2006) Aptamer conformational switch as sensitive electrochemical biosensor for potassium ion recognition. *Chem. Comm.* 3432-3434.
21. Radi, A.-E., Sanchez, J. L. A., Baldrich, E. and O'Sullivan, C. K. (2005b) Reusable impedimetric aptasensor. *Anal. Chem.* **77,** 6320-6323.
22. Rodriguez, M. C. Kawde, A.-N. and Wang, J. (2005) Aptamer biosensor for label-free impedance spectroscopy detection of proteins based on recognition-induced switching of the surface charge. *Chem. Comm.* 4267-4269.
23. Xu, D., Xu, D., Yu, X., Li, Z., He, W. and Ma, Z. (2005) Label-free electrochemical detection for aptamer-based array electrodes. *Anal. Chem.* **77,** 5107-5113.
24. Xu, Y., Yang, L., Ye, X., He, P. and Fang, Y. (2006) An aptamer-based protein biosensor by detecting the amplified impedance signal. *Electroanalysis* **18,** 1449-1456.
25. Cho, M., Lee, S., Han, S.-Y., Park, J.-Y., Rahman, M. A., Shim, Y.-B. and Ban, C. (2006) Electrochemical detection of mismatched DNA using a MutS probe. *Nucleic Acid Res.* **34,** e75.
26. Darain, F., Ban, C. and Shim, Y.-B. (2004b) Development of a new and simple method for the detection of histidine-tagged proteins. *Biosens. Bioelectron.* **20,** 857-863.
27. Darain, F., Park, D. S., Park, J. S. and Shim, Y.-B. (2004a) Development of an immunosensor for the detection of vitellogenin using impedance spectroscopy. *Biosens. Bioelectron.* **19,** 1245-1252.
28. Briggs, D. (1996) *Practical surface analysis: Auger and X-ray photoelectron spectroscopy*. Chap 3. Spectral interpretation. Seah, M. P. (ed), pp. 112-120, Willey & Sons, Chichester, UK.
29. Herman, T. and Patel, D. (2000) Adaptive recognition by nucleic acid aptamers. *Science* **287,** 820-825.
30. Tombelli, S., Minunni, M. and Mascini, M. (2005) Analytical application of aptamers. *Biosens. Bioelectron.* **20,** 2424-2434.